Summer 2019

Dendroclimatology of yellow cedar (Callitropsis nootkatensis) and late Holocene temperature variability on the western slopes of the North Cascades in Washington State

Christopher A. (Chrisopher Anthony) Trinies
Western Washington University, ctrinies@gmail.com

Dendroclimatology of Alaska yellow cedar (*Callitropsis nootkatensis*) in the West Cascades

by

Christopher Anthony Trinies

Accepted in Partial Completion

of the Requirements for the Degree

Master of Science

ADVISORY COMMITTEE

Chair, Dr. Andrew G. Bunn

Dr. James Helfield

Dr. Robert Mitchell

GRADUATE SCHOOL

David L. Patrick, Interim Dean

Master's Thesis

In presenting this thesis in partial fulfillment of the requirements for a masters degree at Western Washington University, I grant to Western Washington University the non-exclusive royalty-free right to archive, reproduce, distribute, and display the thesis in any and all forms, including electronic format, via any digital library mechanisms maintained by WWU.

I represent and warrant this is my original work, and does not infringe or violate any rights of others. I warrant that I have obtained written permissions from the owner of any third party copyrighted material included in these files.

I acknowledge that I retain ownership rights to the copyright of this work, including but not limited to the right to use all or part of this work in future works, such as articles or books. Library users are granted permission for individual, research and non-commercial reproduction of this work for educational purposes only. Any further digital posting of this document requires specific permission from the author.

Any copying or publication of this thesis for commercial purposes, or for financial gain, is not allowed without my written permission

Christopher A. Trinies

August 17, 2019

Dendroclimatology of yellow cedar (*Callitropsis nootkatensis*) and late Holocene temperature variability on the western slopes of the North Cascades in Washington State

A Thesis

Presented to

The Faculty of

Western Washington University

In Partial Fulfillment

Of the Requirements for the Degree

Master of Arts

by

Christopher A. Trinies

August, 2019

Abstract

Subalpine tree growth in the Washington Cascades is often limited by both growing season temperatures and persistence of the winter snowpack, making paleoclimate inferences on temperature alone difficult. Here I expand on three yellow cedar chronologies on the west slopes of the North Cascades and build chronologies for two co-dominant species at one of the sites. I used the VIC hydrologic model to include biologically relevant proxies for water stress, including evapotranspiration deficit, and snow cover in a climate-growth analysis. The co-dominant species, specifically mountain hemlock, showed a climate response reminiscent of a high-elevation, energy-limited environment with an interaction between temperature and winter snow persistence. The first PC of the yellow cedar chronologies showed a strong relationship with growing season minimum temperature ($R^2 = 0.49$), and I did not find a strong correlation with any water stress variables. A temperature reconstruction built with a simple linear model is skillful throughout much of western Washington ($CE > 0.35$) and is consistent with other global and hemispheric reconstructions at low frequencies, differing at the decadal or shorter time scale. This suggests that yellow cedar at these sites may be a useful single-species proxy for temperature on the Pacific slopes of the North Cascades. Having this proxy would be helpful for understanding regional temperature add climate variability as well as adding spatial resolution to global reconstructions that are currently lacking the maritime influence on temperature.

Acknowledgements

I want to thank the undergraduate assistants that helped me prepare some of the cores: : Eric McDougall and Kaylee Spivey. Those that collected and prepared the yellow cedar updates cores before I got started on the project: Nathan Moore, Dustin Gleaves, Jamis Bruening, Tyler Tran, Nicolas Boye, Nick Werner, Gemma Woodhouse, Isaiah Wynters, and Austin Corotan. Caroline, who collected the co-dominant species cores, and Andrew who helped prepare them. Chris Robertson, whose initial work on the species provided the kernel for this project.

Meli, my partner without whom I would never have started down this road and who occasionally kept me fed along the way.

Jim Helfield and Bob Mitchell, whose guidance helped shape my writing and understanding of some of the data products and how they should be interpreted.

And a special thank you to Andy Bunn, who helped shape my understanding of dendrochronology and approach to science in general, and showed patience when I needed it the most. Thank you.

Contents

Abstract **iv**

Acknowledgements **v**

List of Figures **vii**

List of Tables **vii**

Introduction **1**

Methods **4**

Site Description 4

Tree Core and Chronology Development 4

Climate Data 7

Analysis 7

Results **11**

Tree-ring chronologies 11

Site-specific climate correlations 12

Temperature reconstruction 16

Discussion **21**

Literature Cited **27**

Appendix I **35**

List of Figures

1 Site Locations 5
2 Principle component loadings 13
3 yellow cedar site chronologies 14
4 Canyon Lake species chronologies 15
5 yellow cedar climate correlations 17
6 Principle component climate correlations 18
7 Reconstruction skill 19
8 Temperature reconstruction 20
9 Reconstruction - NTREND comparison 20

List of Tables

1 Site characteristics 5
2 Chronology Statistics 11
3 Climate correlation summary 13
4 Tree growth model skill 16

Introduction

Anthropogenic climate change has emerged as perhaps the greatest challenge facing human civilization (IPCC, 2018). As societies reckon with planning, mitigation, and adaptation to variations in climate, the importance of high-resolution paleoclimatology has come to the fore. Paleoclimate proxy data are essential tools for better understanding the dynamics and natural range of variability of past climate (Anchukaitis, 2017). Proxy data from tree-rings and other sources that span the late Holocene have helped us understand how the climate has evolved, especially at global and hemispheric scales. By relating proxy data to past climates we have gained valuable insights into the relative importance of natural and anthropogenic climate forcings, and these insights have helped inform our models of future climate (Hegerl et al., 2006; Schurer et al., 2014). The span of time covered by many proxy data, much longer than any instrumental record, can be used to infer how circulation patterns that cycle on a scale of decades to centuries may contribute to the natural climate variability (Coats et al., 2016).

At regional scales, we have often lacked the necessary paleoclimate proxy data to make strong inference about late Holocene climate variability or to reconstruct variables of particular interest like temperature. Although skillful at the hemispheric scale, when local data are not available the reconstruction target is based on data from distant proxies that may experience subtle or stark differences in climate. This results in an understanding of local climate that does not reflect the true range or variation in climate over time (St. George, 2014). For instance, the best current models for late Holocene temperature variability in the Northern Hemisphere are from the recent Northern Hemisphere temperature reconstruction (NTREND) (Wilson et al., 2016). In this reconstruction, a large portion of North America was represented by one or two proxy chronologies. These are not evenly distributed and there are large spatial gaps which limits our understanding of regional climate variability. For these underrepresented regions, lack of a local proxy results in a weakened

understanding of local and regional conditions, and impacts the NTREND model as a whole.

The Pacific Northwest of the conterminous United States is one such area where we know little about the local temperature variability over the last millennium, particularly west of the Cascade Mountains. The lack of temperature proxies in this region stems in part from the unique mix of climate diversity within a small spatial extent (Mass, 2008). Proximity to the Pacific Ocean acts to buffer temperatures west of the Cascades, leading to a smaller diurnal and seasonal temperature variations than those experienced on the eastern slopes or other areas influenced by a continental climate regime (Franklin and Dyrness, 1973). The Cascades also provide a topographic break between the mesic west and dry east, and western lowland precipitation is itself often moderated by the rainshadow cast by the coastal Olympic Mountains, a phenomena that varies spatially by the track of any one particular storm system. The best climate proxies in the region stem from the water-limited eastern Washington. At high elevations, where temperature-limited growing conditions would be expected (Körner, 2012), winter snowpack is often as strong a factor in limiting growth as summer temperatures (Peterson and Peterson, 2001). The result is that in large scale temperature reconstructions like the NTREND ensemble, the Pacific Northwest is represented by proxies from higher latitudes and the continental interior, where temperatures more reliably limit summer tree growth.

Given these challenges to finding suitable proxy data for temperature variations in the region, it becomes a question of weather a skillful one exists. Most prior research in the region has failed to separate the influence of winter snowpack from summer temperatures on annual tree growth. Most of the high-elevation species that have been studied, including mountain hemlock (*Tsuga mertensiana* (Bong.) Carrière), subalpine fir (*Abies lasiocarpa* (Hook.) Nutt.), and lodgepole pine (*Pinus contorta* Douglas ex Loudon), show a temperature sensitivity that is heavily moderated by either winter snowpack or growing-season moisture availability (Peterson and Peterson, 2001; Peterson et al., 2002; Case and Peterson, 2007). Douglas-fir (*Pseudotsuga menziesii* (Mirib.) Franco.) and ponderosa pine (*Pinus ponderosa* P. Lawson & C. Lawson), two other common species in the region, tend to exhibit a sensitivity to water availability without the temperature relationship, or with a negative relationship to summer temperatures that is more indicative of water stress (Littell et al., 2008; Kusnierczyk and Ettl, 2002). Where a temperature reconstruction has been attempted, it involves a more complicated process using multiple species to separate out the temperature signal

from other signals (e.g., Graumlich and Brubaker, 1986), which might lead to greater uncertainty. One species that has shown sensitivity to summer temperatures without the winter precipitation limitation is yellow cedar (*Callitropsis nootkatensis* (D. Don) D. P. Little), but that species has not been intensively studied in a dendroclimatological context (Laroque and Smith, 1999; Robertson, 2011). The current focus of yellow cedar research in relation to climate has been on the recent decline of stands in Southeast Alaska (e.g., Beier et al., 2008; Barrett and Pattison, 2017; Bidlack et al., 2017). However, the noted decline has been linked more strongly to a lack of insulating snow cover rather than warming temperatures, and those dynamics do not appear to be present in the North Cascades (Hennon et al., 2006, 2016).

The objectives of this study are two-fold. First, I will establish whether it is possible to develop yellow cedar as a temperature-sensitive dendroclimatic proxy on the western slopes of the North Cascades to reconstruct regional summer temperatures over the last 500+ years. To do this, I will update three existing, unpublished yellow cedar chronologies from the northwest Cascades at Canyon Lake, Grouse Butte and Mount Pilchuck. Because yellow cedar has not been extensively studied in the context of peleoclimate and because temperature limitations are often compounded by water stress, I will also develop chronologies from two co-dominant species at Canyon Lake, mountain hemlock and Pacific silver fir (*Abies amabilis* Douglas ex J. Forbes), to compare the possible range of limiting factors to growth across species. Second, if yellow cedar is a suitable proxy for temperatures in the North cascades I will use the climate-growth relationship to reconstruct temperature variability at each site and through a broader spatial reconstruction throughout the region.

Methods

Site Description

The three study sites of Canyon Lake, Grouse Butte, and Mount Pilchuck are in mid-elevation montane forests on the mesic western slopes of the northern Cascade Mountains in Washington State (Figure 1; Table 1). The sites are in the mixed conifer zone with yellow cedar co-located with other species including mountain hemlock and Pacific silver fir.

Regional weather patterns are dominated by the Pacific maritime climate, typified by cool, moist winters and a generally dry growing season, with winter precipitation predominantly falling as snow above 1000 m (Franklin and Dyrness, 1973). Minimum site temperatures are below freezing from mid-November through mid-April, and generally don't reach 5°C until June (PRISM Climate Group, 2019). Annual precipitation exceeds 260 cm at each site, with more than 80% falling during the non-growing season between October and May. Each site is steep with rocky, well-drained soil and at an elevation of about 1000 m. These sites were chosen for the presence of yellow cedar growing in stands with exceptional ages. These sites have yellow cedar that were not logged and are typically on slopes that are too steep and high in elevation to have been logged in the 20^{th} century. The fire-return interval here is typically in excess of 1000 years, which allows the establishment of old-growth stands like these (Franklin and Hemstrom, 1981; LANDFIRE, 2014). For example, the most recent stand-replacement fire at the Canyon Lake site was c1170 CE, and the predominant disturbance type at the site is due to wind events (Agee and Vaughn, 1993).

Tree Core and Chronology Development

I updated existing yellow cedar chronologies that were collected in 2010 by Robertson (2011) and augmented them with additional samples from the same sites in 2015. Tree Cores from two co-dominant species, Pacific silver fir and mountain hemlock, were collected from the Upper Canyon

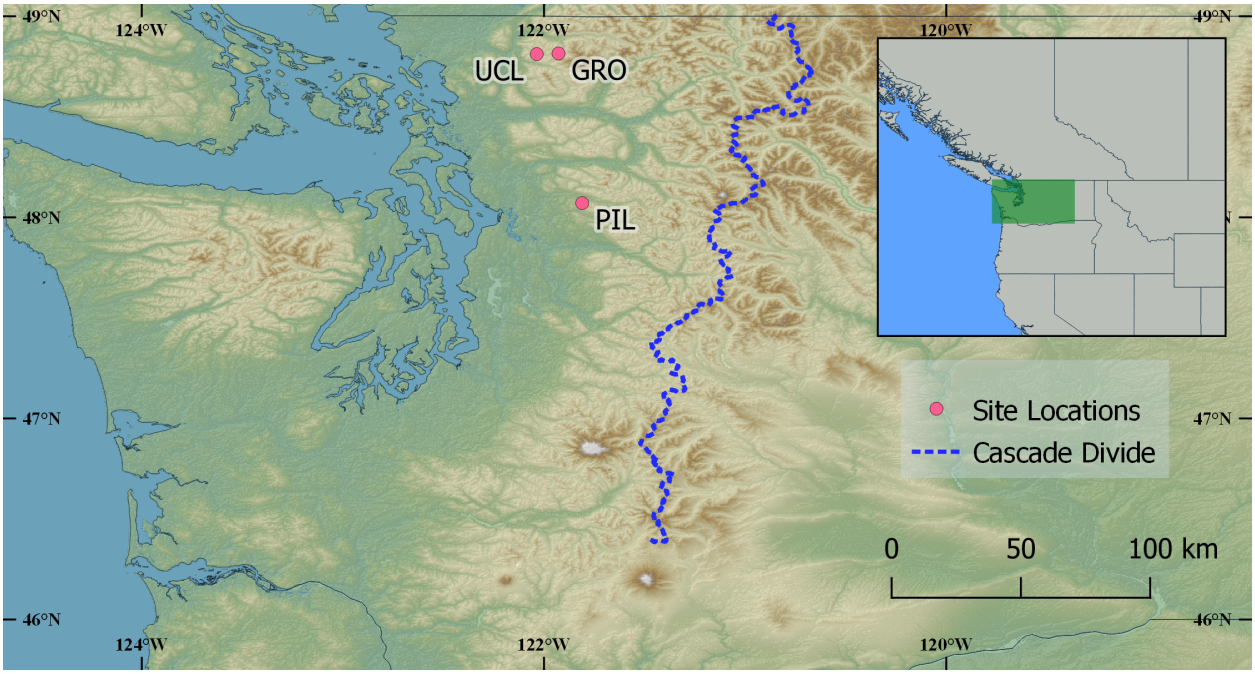

Figure 1: Site locations within the Washington Cascades: Upper Canyon Lake (UCL), Grouse Butte (GRO), and Mount Pilchuck (PIL). Yellow cedar chronologies were built at each of the three sites, with silver fir and mountain hemlock chronologies developed at Canyon Lake.

Table 1: Coordinates and topographic position of each of the three yellow cedar study sites. Data from Robertson (2011).

	Latitude	Longitude	Aspect	Elevation (m)
Canyon Lake	48.8119	-122.0361	NNW	1310-1402
Grouse Butte	48.8150	-121.9281	NNE	1219-1341
Mount Pilchuck	48.0708	-121.8103	N	944-1005

Lake site in the early summer of 2016. All samples were prepared using standard dendrochronologic techniques (Stokes and Smiley, 1968; Cook and Kairiukstis, 1990). Trees were selected for their position in the canopy structure, with care taken to ensure that no trees with visible damage were selected during the initial sampling. Later field work involved coring an increasing number of trees, including some that had a minimal amount of visible scarring or other signs of disturbance. Two cores were taken per tree wherever feasible, and the cores were air-dried, mounted, and sanded with increasingly finer grit sandpaper so that individual cells within each ring were clearly visible. I used a Velmex sliding stage to measure ring widths to the nearest 0.001 mm, and crossdated them visually and statistically by site and species (Bunn, 2010).

To maintain low-frequency trends while removing age-specific growth patterns, I detrended each yellow cedar core using a modified negative exponential growth curve or straight line (Fritts et al., 1969). When the presence of juvenile growth prevented the establishment of a suitable curve, I used a Hugershoff curve to remove those artifacts of juvenile growth from the chronology (Warren, 1980). I used a bi-weight robust mean to estimate the mean chronology for each site and species, truncating the chronologies at a sample depth of five to ensure adequate sample depth. Summary statistics, including the mean interseries correlation ($\bar{r}$), expressed population signal (EPS), and subsample signal strength (SSS), were calculated for each of the chronologies. The interseries correlation is calculated by removing each core from the chronology and correlating it to the remaining chronology over the common interval. Expressed population signal and subsample signal strength are both measures of the strength of a common signal. EPS (eq. 1) is a ratio of the mean interserries correlation times the number of trees in the chronology to he same modified by the difference between the mean interserries correlation and one, and is used as an estimate of how well the chronology represents the true population. SSS (eq. 2) is the ratio of the EPS of the chronology to the EPS at a single time, given the number of cores at that particular time and represents the robustness of a chronology going back in time (Cook and Kairiukstis, 1990; Buras, 2017).

$$(1)\ \mathrm{EPS} = \frac{t\bar{r}}{t\bar{r} + (1 - \bar{r})} \qquad (2)\ \mathrm{SSS} = \frac{\mathrm{EPS}(t)}{\mathrm{EPS}(t_i)}$$

Climate Data

I used output from the variable infiltration capacity (VIC) hydrologic model in order to model physiologically relevant stressors on tree growth (Liang et al., 1994). The VIC model is a multiple soil-level hydrologic model, generally developed to couple global climate modeling with finer-scale local resolution modeling. I used output from a model run set up by the Climate Impacts Group for the purpose of modeling future regional streamflow conditions (Hamlet et al., 2012). They used a $1/16^{th}$ degree resolution ($\sim 6\,\text{km}$) run in the Colombia River and adjacent Puget Sound Basins, calibrated to Columbia River main stem and tributary stream flow. Temperatures for these data were derived from regional meteorologic station data and modeled using the PRISM method for interpolation over complex terrain (Daly et al., 1994). Output was calibrated to streamflow using station data primarily along the Colombia River and associated tributaries. I also used the $1/24^{th}$ degree resolution ($\sim 4\,\text{km}$) Parameter-elevation Regressions on Independent Slopes (PRISM) data set to compare results and for my reconstructions (Daly et al., 2002). The PRISM data have been successfully used in many studies of tree growth and climate in areas of complex terrain (e.g., Salzer et al., 2009; Williams et al., 2010; Biondi et al., 2014; Evans et al., 2017, etc.). The VIC data run from 1915-2007, with the first few years used to "spin up" and calibrate the model output. The PRISM data for this region start in 1895 and continue through the present.

Analysis

Site-Specific Climate Correlations

I aggregated the daily VIC data into monthly variables for each grid cell that corresponded to a site location. For energy-limitation comparisons I used the average minimum and maximum daily temperatures, along with monthly mean snow-water equivalent (SWE). Mean soil moisture and total monthly precipitation were used as proxies for water stress, and I also looked at evapotranspiration deficit (DEF), which is the difference between actual and potential evapotranspiration (AET-PET) (Stephenson, 1998; Littell et al., 2008). I ran a bootstrapped monthly climate correlation analysis, using climate data form the previous year's (py) growing season (py-May) through the end of the current year (cy) growing season (cy-September) compared against yearly growth

(Biondi and Waikul, 2004). Without a means to quantify the uncertainty in the VIC model output, I compared the correlation results to other published climate-growth responses with a focus on mountain hemlock, which has been extensively studied in the region. As an additional means to compare model results, I ran the same analysis using the monthly PRISM data. Because the soil moisture, ET, and SWE parameters are not available through the PRISM model, I included vapor pressure deficit in my VIC analysis as a comparison tool. For the Canyon Lake chronologies I ran a principle components analysis to separate out species-dependent differences in the climate-growth response. As a way to isolate the climate effects of variables that covary through time, I analyzed the residuals of a partial correlation for independent correlations. Finally, I used the correlation results to inform a partial regression between yellow cedar and climate to further refine my climate-growth relationship inferences.

For each site chronology I looked at correlations between climate and tree growth, using monthly climate data. I used those results to inform a regression model to look at the relative importance of the correlated climate variables, and fed those results into a predictive model. The predictive model looked at tree growth as a function of climate. I cross-validated the model using a 10-fold cross validation process, whereby I randomly sliced the data into ten-year segments in order to preserve the autocorrelation structure and trained ten models, each one withholding one of the segments. For each model run, I calculated the reduction of error (RE), coefficient of efficiency (CE), mean squared error (MSE), and coefficient of determination (R^2) of the calibration period, and calculated the mean of these values as the model statistics. Reduction of error (eq. 3) is a ratio of the error in the validation period to the error as compared to the mean during the calibration period, and the coefficient of efficiency (eq. 4) is the error in the validation as compared to the mean during the validation period (Cook and Kairiukstis, 1990; Cook et al., 1999). Values above zero suggest that the model does better than a random expectation in predicting the target. I ran this process 1000 times, and took the median of the model runs as my overall statistics. I analyzed the model residuals for autocorrelation structure, and used a Breusch-Pagan test for heteroskedasticity.

$$(3)\ \mathrm{RE} = 1 - \frac{\sum (x_i - \hat{x}_i)^2}{\sum (x_i - \bar{x}_c)^2} \qquad (4)\ \mathrm{CE} = 1 - \frac{\sum (x_i - \hat{x}_i)^2}{\sum (x_i - \bar{x}_v)^2}$$

Regional Climate Reconstruction

When reconstructing some climate parameters when using tree growth as a proxy, it is most common to use one point of data that is more or less representative of the climate at that particular site, or a regional mean for multi-site proxies. Those models generally take data from multiple stations and interpolate them into the empty cells, making it possible to model conditions without a local weather station. But those relationships may break down when the climate model fails to capture key topographic features that can have a large impact on local growing conditions, or when the site chronology is located in a small microhabitat that is not representative of the surrounding topography. As a way to simultaneously test my assumptions about the relationship between yellow cedar growth and climate, and to test the spatial integrity of a reconstruction, I used spatially distributed climate data and built a climate reconstruction at each grid cell, taking note of the model statistics as a function of space. The standard climate data to use for a reconstruction in this region is the PRISM model, which interpolates climate in topographically complex terrain and is routinely validated and kept up to date (Daly et al., 2002). I used the fine-scale PRISM model to build a spatially explicit model of temperature variability throughout the region. To incorporate each of the three chronologies while reducing the covariance associated with them, I used the first principle component of the three yellow cedar chronologies as my temperature proxy. Because neither the temperature data nor the tree-ring chronologies are a stationary time series, I ran bootstrapped 10-fold cross-validation of a linear single-variable regression model, with a random removal of the predicted values. For each grid cell I calculated the median R^2 of the regression, RE, CE, and MSE.

To validate my reconstruction results I compared the tree-ring series and the general reconstruction to the NTREND regional reconstruction and the tree-ring series that most heavily influenced the local grid cell, as well as the regional data from which the NTREND reconstruction was built. I used a simple correlation between each of these and both the reconstruction and the local climate models. To look specifically at lower frequency variations I did the same for the five-year spline of each model, which removes the high-frequency variation by using a local polynomial to fit the data. A spline is a standard way of filtering out high-frequency signals while retaining lower-frequency variations. I also compared the reconstruction to published results from other temperature recon-

structions that cover the same region, using the 1951-1990 climate normal as a reference time frame. A climate normal is a thirty-year period over which climatological variables, including temperature, are averaged and is a standard means of comparing climate over time.

My analysis relied heavily on the open source software R version 3.5 (R Core Team, 2019) and the associated packages dplR (Bunn, 2008), treeclim (Zang and Biondi, 2015), and raster (Hijmans, 2019). Maps were created using QGIS software (QGIS Development Team, 2018). A full list of software and packages used can be found in Appendix II.

Results

Tree-ring chronologies

I built a total of five tree-ring chronologies from three sites and three species (Table 2). There were a total of 68 cores from 35 trees added to the existing yellow cedar chronologies, and a total of 30 additional cores from the co-dominant species at Upper Canyon Lake that were successfully crossdated (i.e., accurate dates were assigned to each ring). The oldest cores date back prior to 1100 at the Mount Pilchuck site and Grouse Butte, though only a few cores from each site go back that far. The chronologies from the co-dominant species were much shorter, only reaching back to the mid-eighteenth century. Overall, the yellow cedar showed a strong interserries correlation and first-order autocorrelation ($\bar{r} > 0.5,\ \text{AR}(1) > 0.75$), as well as a strong shared signal within each site as seen wuth the EPS over 0.85 throughout (Table 2).

The three mean site chronologies for the yellow cedar are each more than 750 years in length, with a strong shared signal going back to 1300 CE (Figure 3). Each of the Canyon Lake species cross-dated with one another, and there was a great deal of agreement between yellow cedar at each

Table 2: Select chronology statistics for each of the three species at Canyon Lake, and the two additional yellow cedar sites. Though two cores were collected from each tree sampled, not all cores successfully crossdated with the master chronology. Mean Age refers to the average number of discernible years in a core, and the time span shows the length of coverage at a site by at least one tree core. Also included are the mean interseries correlation ($\bar{r}$), mean first-order autocorrelation (AR-1), and the expressed population signal (EPS) of the chronology.

				Mean	Time Span		Mean	Mean	
Site	Species	Trees	Cores	Age (yrs)	Start	End	$\bar{r}$	AR-1	EPS
Canyon Lake	CANO	28	50	503	1221	2015	0.64	0.81	0.94
Canyon Lake	TSME	6	12	277	1707	2015	0.59	0.76	0.86
Canyon Lake	ABAM	9	18	295	1689	2015	0.68	0.76	0.92
Grouse Butte	CANO	21	37	519	1067	2015	0.56	0.83	0.88
Mount Pilchuck	CANO	27	53	589	1075	2015	0.57	0.87	0.94

of the sites. The yellow cedar mean site chronologies also correlated well to each other ($r > 0.7$), as did the co-dominant species at Canyon Lake ($r = 0.75$) though the correlations between yellow cedar and the other species were not as strong ($r < 0.46$). Each of the site chronologies has a strong common signal throughout the 20^{th} century (Figure 4). The first principle component of the CANO, ABAM, and TSME at Canyon Lake explained about 69% of the variance (Table 2) with moderate differences in the loadings between species. The second principle component explained about 26% of the variance with greater difference in the loadings between species.

Site-specific climate correlations

yellow cedar showed a strong relationship with growing-season and previous year minimum temperatures at each of the sites, and an inverse relationship with winter snowpack at Canyon Lake and Grouse Butte, the two northern sites (Figure 5). Mountain hemlock also showed a strong relationship with growing-season temperatures, and shared the negative relationship to winter snowpack with both the yellow cedar and silver fir. None of the chronologies showed a consistent seasonal sensitivity to precipitation. There are weak relationships with winter maximum temperatures and vapor pressure deficit exist but these are not consistent across sites or species. Partial correlation results show that temperatures are still correlated with growth when winter snow is held constant, but the SWE-growth relationship is not apparent given constant temperatures. The first principle component of the yellow cedar chronologies showed the same sensitivities as did each of the individual chronologies, as did the first PC of the three species at Canyon Lake (Figure 6). The second PC of the three-species chronologies also shows a sensitivity to summer temperatures but not to winter snowpack. It also includes a sensitivity to summer VPD and DEF, a correlation not present in any of the other monthly correlation analyses. Correlations with the PRISM data show similar results, and are not presented here.

The PRISM minimum temperature data was able to model tree growth with some skill at each of the sites. The Mount Pilchuck site produced the strongest model, with the R^2 of the reconstruction at nearly 0.5 and CE = 0.40, and the weaker Grouse Butte site still had a CE of 0.15 (Table 4). A residual analysis showed no lingering autocorrlative structure, and the residuals were homoskedastic in each of the three models.

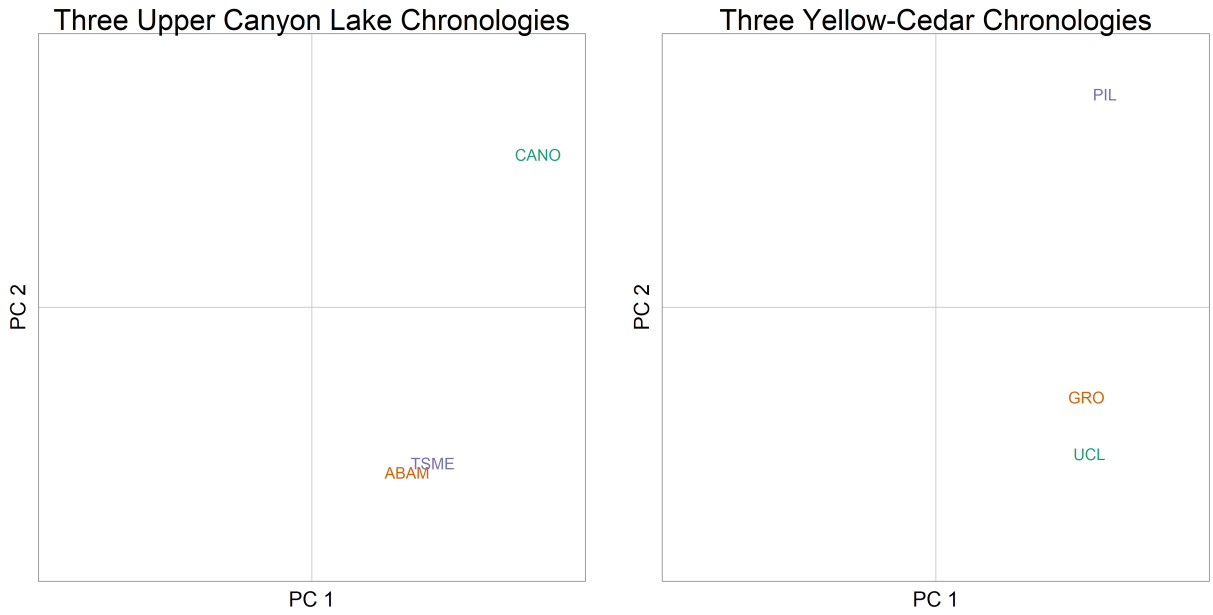

Figure 2: Principle component loadings for each of the chronology composites. On the left are the three Canyon Lake species, and on the right are the loadings for the three yellow cedar chronologies. Only loadings with more than 5% explained variance are shown. For the Canyon Lake chronologies, the first principle component explains 69% of the variance, and the second principle component explains 26% of the variance. For the three yellow cedar chronologies, the first two principle components explain 85% and 10% respectively.

Table 3: Summary table for the bootstrapped climate correlation results. Positive (+) or negative (−) correlations shown all persist for 2+ consecutive months and only represent the correlations that exist across species or site and have a reasonable physiological basis. Shown here are minimum and maximum summer (JJA) temperature, spring (MAM) evapotranspiration deficit (DEF), winter (NDJFM) snow water equivalent (SWE), and water-year precipitation (October-September). Previous year correlations are identified "py-" with the exception of winter SWE, which represents the winter prior to a growing season. Negative correlation with winter SWE for Grouse Bute and Mount Pilchuck (∗) are ony signfiicant for the spring months.

	Mountain	Silver	yellow cedar			Three-species		Three-site
	Hemlock	Fir	Canyon	Grouse	Pilchuck	PC-1	PC-2	PC-1
Summer T Min	+		+	+	+	+	+	+
py-Summer T Min	+		+	+	+	+	+	+
Summer T Maxn	+	+						
py-Summer T Max	−	−				−		
Spring DEF	−		−			−		
py-Spring DEF	−		−			−		
Winter SWE	−	−	−	∗	∗	−		−
Water-year Precip								

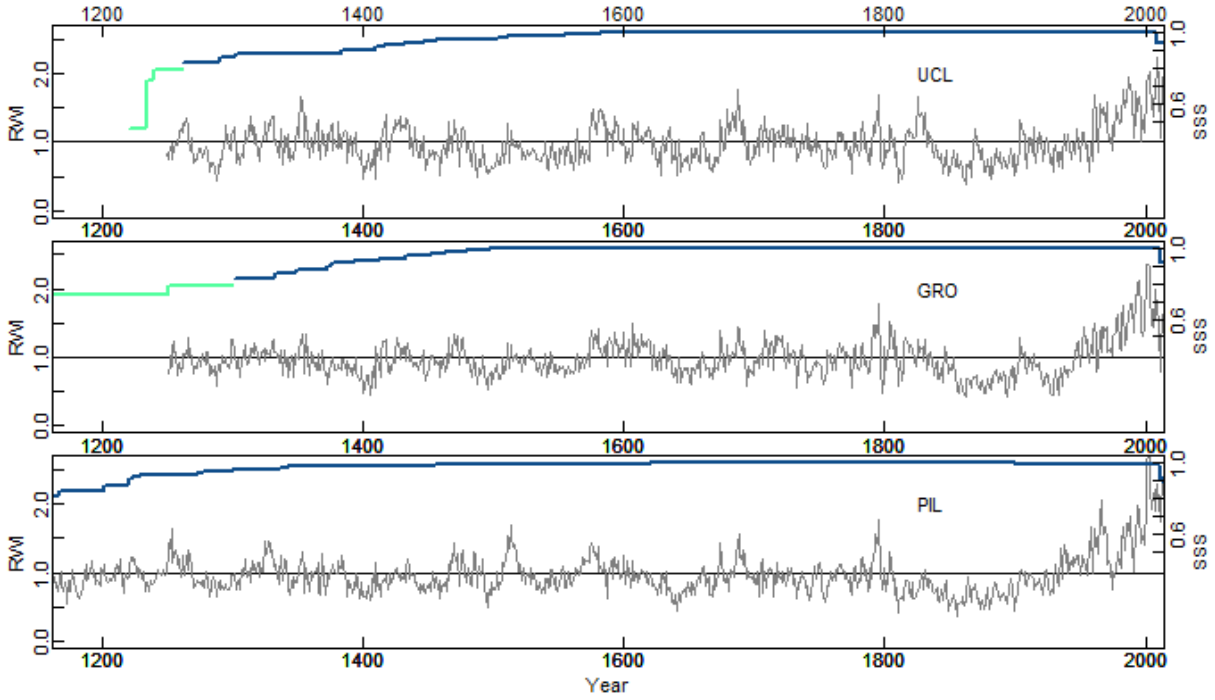

Figure 3: Site chronologies for the detrended yellow cedar series. Each chronology is represented by at least five tree cores. Also included is the running subsample signal strength (SSS). An SSS below 0.8 is shown in light green, and denotes the part of the chronology that is not used for the reconstruction. Where SSS is shown but not the mean site chronology, the chronology would be represented by fewer than five samples, and is not shown. An SSS greater that 0.8 is shown in dark blue.

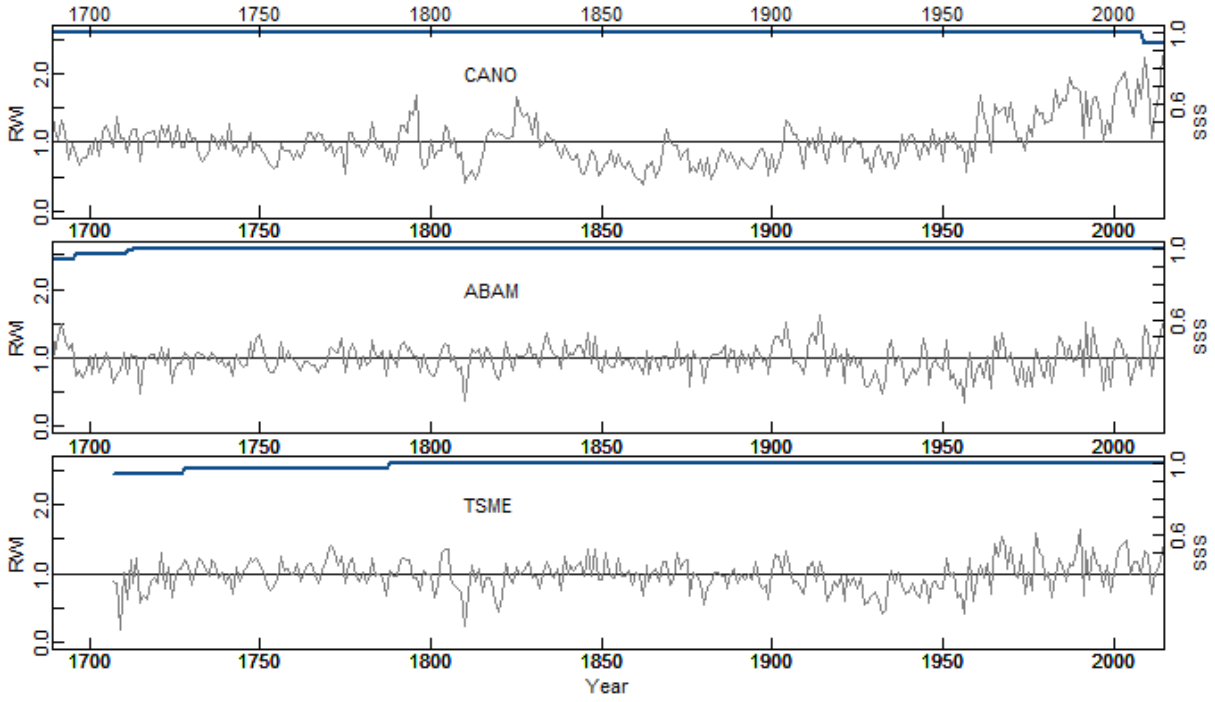

Figure 4: Species chronologies for each of the detrended species-specific series at Canyon Lake. Each chronology is represented by at least five tree cores. Also included is the running subsample signal strength (SSS). An SSS greater that 0.8 is shown in dark blue. There is no part of either series in this time frame where the SSS is below 0.8.

Table 4: Model statistics for tree growth as a function of growing-season temperatures at each of the three sites. Shown here are the R^2 of the reconstruction, reduction of error (RE), coefficient of efficiency (CE), and mean squared error of the reconstruction (MSE).

	R^2	RE	CE	MSE
Canyon Lake	0.41	0.33	0.30	0.10
Grouse Butte	0.27	0.19	0.15	0.16
Mount Pilchuck	0.49	0.42	0.40	0.13

Temperature reconstruction

There is a high degree of variability in the reconstruction skill by cells, with the mean model RE ranging from below 0 to more than 0.5 (Figure 7). A majority of the high-skill cells appear to be located in the lower elevation areas surrounding the Puget Sound, and the weakest relationships are on the east slopes of the Cascades and west of the Olympic Peninsula. Reconstruction results from the higher-skill areas near the sample sites show variations in temperature over the last 600 years that are generally below the 1951-1990 climate normal (Figure 8). This suggests that temperatures were 1-2 °C cooler during the Little Ice Age, with periods in the late 16^{th} and late 17^{th} centuries during which temperatures may have approached current conditions, though only for a few years each time. The residuals from these high-skill cells do have some lingering autocorralitive structure, but are still homoskedastic. The reconstruction compares favorably with the NTREND reconstruction over the 20^{th} century, though there is more variability in this one prior to the 18^{th} century (Figure 9). The NTREND reconstruction correlates overall with UCL CANO at $r = 0.34$, but over the 1895-2014 time period the Pearson's correlation coefficient is 0.56.

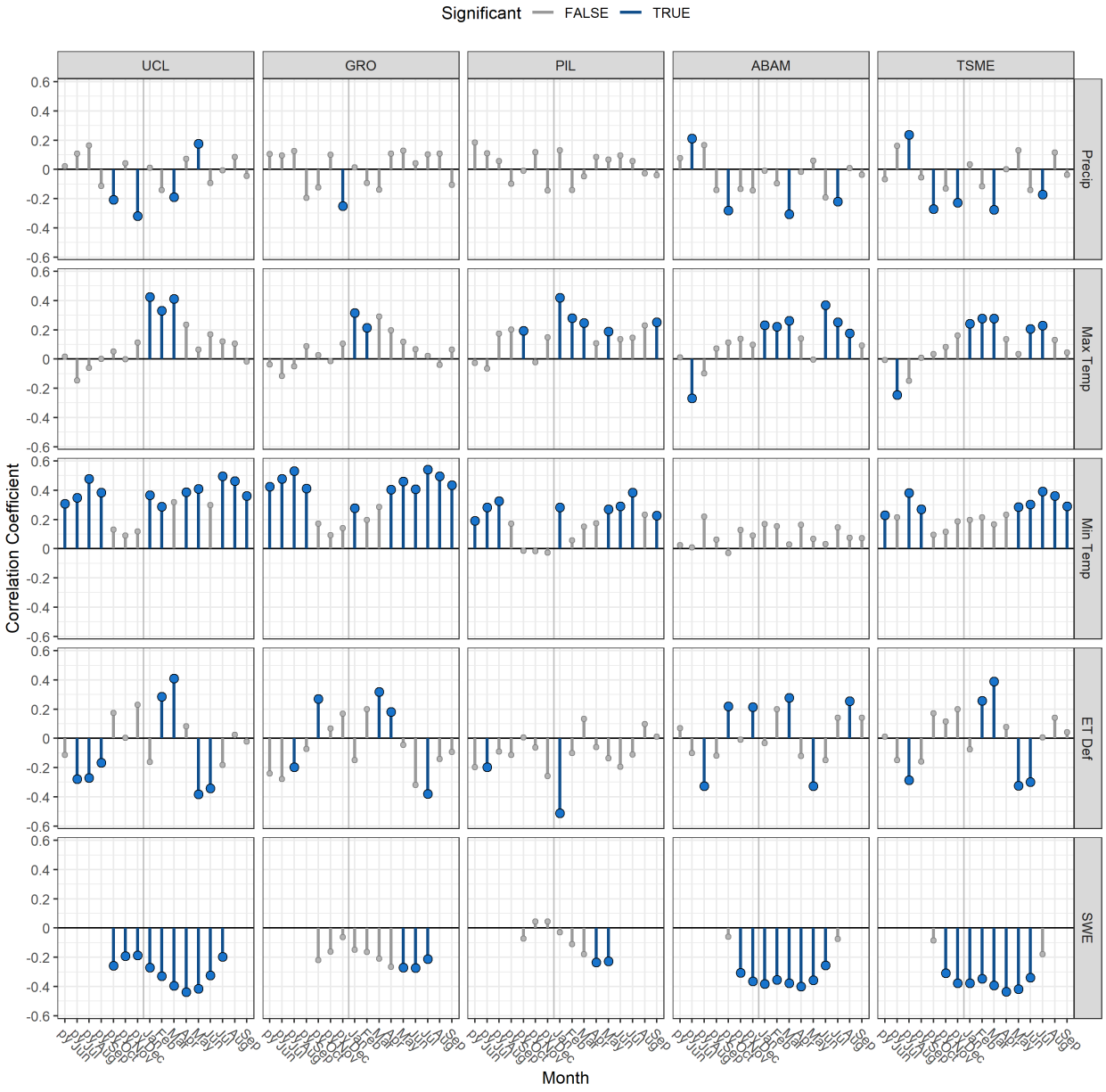

Figure 5: Monthly bootstrapped climate correlations between each of the chronologies and select monthly climate variables from the VIC model. yellow cedar chronologies are from Canyon Lake (UCL), Grouse Butte (GRO), and Mount Pilchuck (PIL). Mountain hemlock (TSME) and Pacific silver fir (ABAM) chronologies are from Canyon Lake. Monthly climate variables shown are total precipitation, average daily maximum and minimum temperatures, total monthly evapotranspration deficit (ET Def), and first of the month snow-water equivalent (SWE). Bootstrapped monthly climate correlations are calculated for each month from June of the previous year through September of the current year, compared against each year of tree growth. Direction and strength of all correlations are shown, with the non-significant correlations in (light) grey.

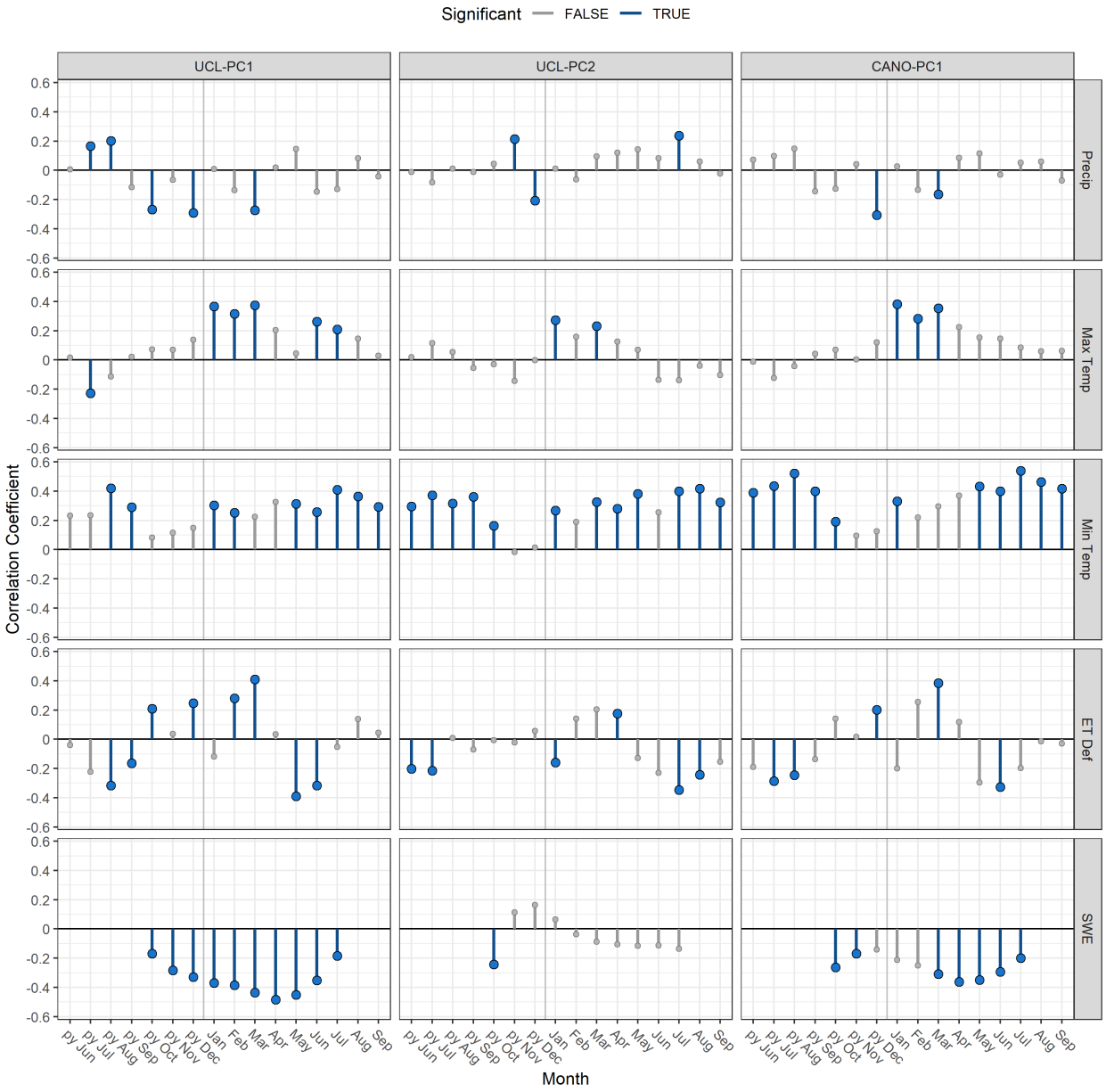

Figure 6: Monthly bootstrapped climate correlations between the first and second PC for the three species at Canyon Lake (UCL-PC1 & UCL-PC2), and first PC of the three sites chronologies for yellow cedar (CANO-PC1), compared against the VIC climate model output. Monthly climate variables shown are total precipitation, average daily maximum and minimum temperatures, total monthly evapotranspration deficit (ET Def), and first of the month snow-water equivalent (SWE). Bootstrapped monthly climate correlations are calculated for each month from June of the previous year through September of the current year, compared against each year of tree growth. Direction and strength of all correlations are shown, with the non-significant correlations in (light) grey.

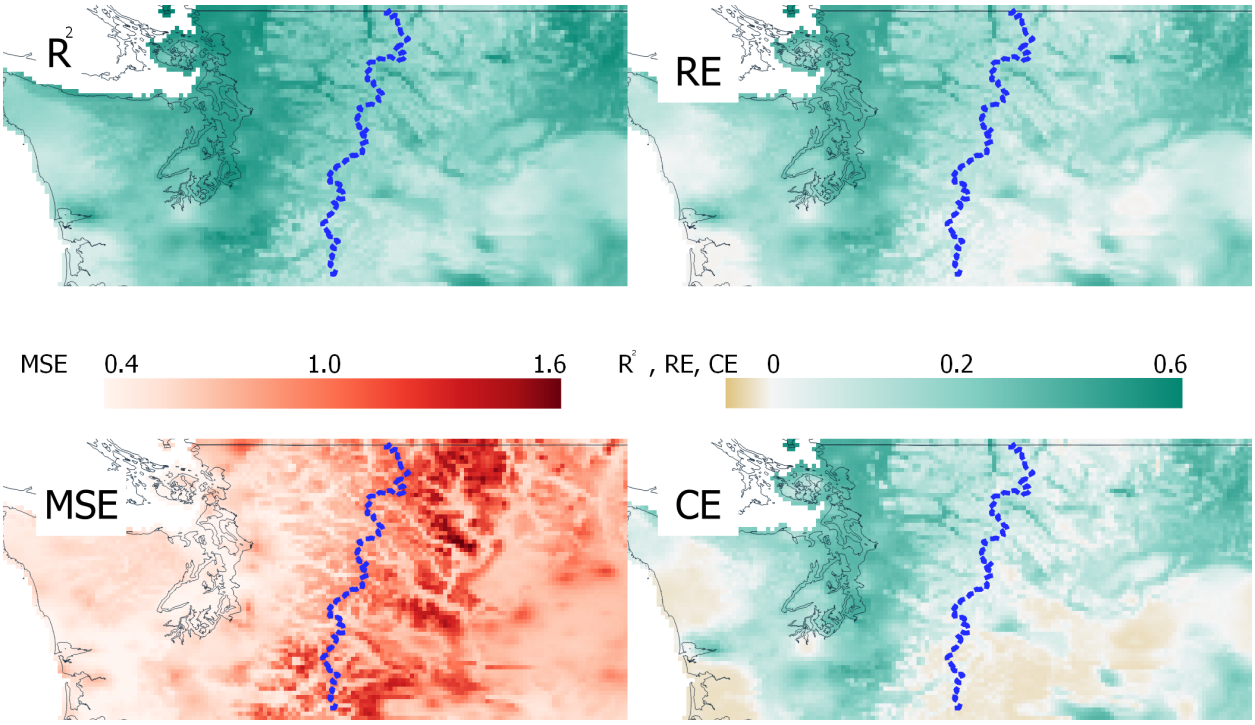

Figure 7: Skill metrics of a minimum summer temperature reconstruction applied at each grid point in the north Cascades, WA. The temperature target is derived from the $1/24^{th}$ degree spatial resolution PRISM historical climate model, and represents the mean daily June-August temperatures. The first principle component of three regional yellow cedar site chronologies was used as the proxy. These metrics are from the bootstrapped 10-fold cross validation of a linear model. Shown here are the R^2 of the reconstruction, RE, CE, and MSE of the reconstruction. The model was applied individually at each cell.

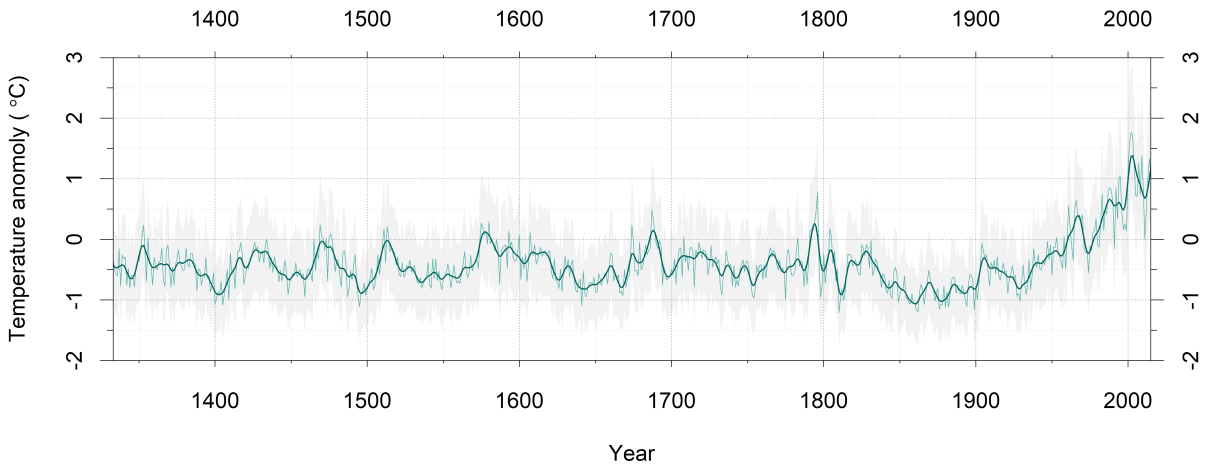

Figure 8: Reconstructed minimum summer temperature anomalies compared to the 1951-1980 climate normal. This reconstruction is derived from the first principle component of the three yellow cedar site chronologies, and the temperature target is mean minimum summer PRISM temperatures, pulled from a representative high-skill grid cell. The error shown is 2× the model MSE of the reconstruction, plus the error in the estimate of the regression. Also shown is a ten-year spline for the reconstruction.

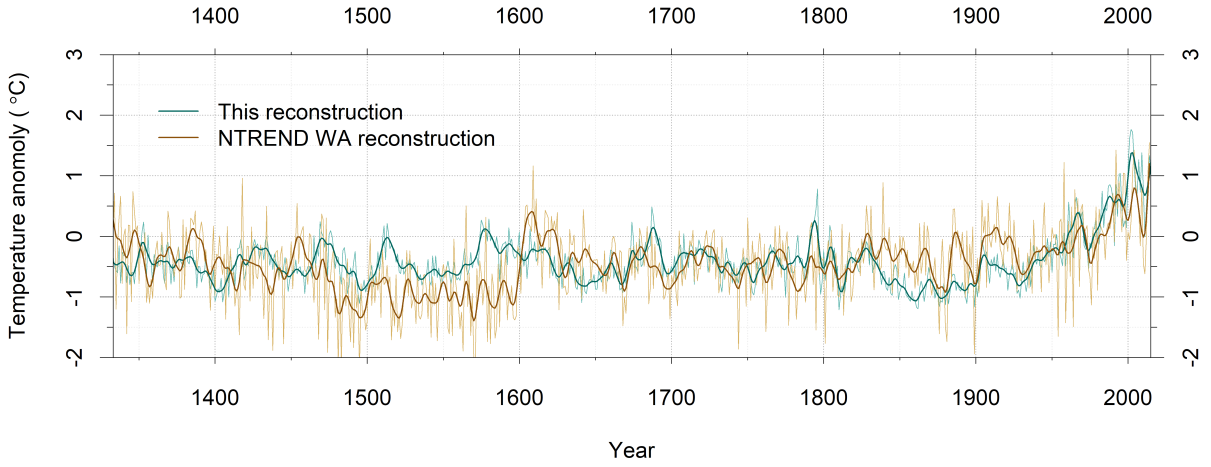

Figure 9: Temperature reconstruction of the west slopes of the Washington Cascades compared against the NTREND ensemble reconstruction for the grid cell representing Washington State, shown as departure from the 1951-1980 climate normal. The thick line represents a ten-year spline for each reconstruction. Western Washington reconstruction is built from three yellow cedar chronologies in the northwest Cascade Mountains, and the NTREND reconstruction is primarily built from chronologies located in Idaho and Alberta, Canada.

Discussion

This study has shown that yellow cedar at these three sites on western slopes in the North Cascades are sensitive to growing season temperatures. A positive correlation with winter temperatures and negative relationship to winter SWE are related more to the covariance with summer temperature than any winter climate response. Using the VIC hydrologic model, I was also able to show that, though yellow cedar is primarily limited by summer temperatures, the temperature signal among co-dominant species at the same sites may be moderated by both winter snowpack and summer water stress. The temperature-growth relationship among yellow cedar can be used to successfully reconstruct temperatures from about 1300 CE through 2015, and the skill of that model varies in the region in a spatially-coherent pattern. This fine-scale look at regional temperature variability can be an important addition to larger regional and hemispheric temperature reconstructions, adding a measure of variability currently lacking in these models.

High-frequency variations in growth can be seen as primarily representing the interannual variations in climate and stand dynamics, with the low-frequency trend in yellow cedar growth enhancing the relationship with growing-season temperatures. The stand-level agreement between each of the three species at Canyon Lake shows that they share a high degree of interannual variance, and this is also born out by the common loading of each species in the first principle component (Table 2, Figure 4). The temperature correlations found in yellow cedar relate more to the remaining, low-frequency variance similar to the third PC from Wilson and Luckman (2002). A stringer relationship between temperature and growth at low frequancies rather than at interannual time steps is similar to results from higher latitudes in North America. At those latitudes, maximum latewood density (MXD) is often a stronger predictor of summer temperatures than ring-width alone (e.g., D'Arrigo et al., 1992; Luckman et al., 1997; Wilson and Luckman, 2003). This is also similar to results from eastern North America, where ring-width does not consistently track tem-

perature while ring density does (Heeter et al., 2019). However, there are no known studies of MXD for yellow cedar at any location, and no studies that used MXD as a climate proxy for other species in the Cascades to compare these results to directly. Crown and Parker (1979) measured MXD in Douglas-fir in the Cascades, but in a plantation context. Retaining the low-frequency variation was an important part of identifying the temperature-growth relationship in part because we lacked density measurements as a comparison tool. This was made possible by not removing the autocorrelation structure in the tree-ring data, which likely retained valuable information (see Razavi and Vogel, 2018). Removing the autocorrelation would have rendered each time series as a stationary (i.e. with a constant mean value) time series, removing the real and common lower frequency trends.

Temperature sensitivity among yellow cedar at the study sites can be seen in the correlation results and confirmed through the three-species model. Although covariance between summer temperatures and winter snowpack at the three sites makes it difficult to separate out the respective influence of each on annual growth, additive models tend to show temperature as having a stronger influence. Additionally, the loss of a significant correlation with SWE—temperature in the partial regression suggests that the SWE-growth relationship is largely an effect of the SWE-temperature covariance. The winter SWE signal is much stronger at the higher elevation Canyon Lake site, while the temperature correlations persist at each of the sites (Figure 5). Interestingly, the Mount Pilchuck chronology showed a stronger correlation with temperatures from the other two sites, and with the PRISM data from Mount Pilchuck, than with the local VIC data. The common growth patterns across sites, represented by the first PC of the chronologies, can be seen as tracking the temperature variation more than any of the stand-level dynamics, and temperature correlations are very strong as well (Figure 6). The first PC of the three species model shares this trend, as it incorporates both the low-frequency variation in yellow cedar growth as well as the site-level high-frequency variation (Table 2). However, the separation seen in the second PC seems to indicate that yellow cedar and the other two species respond differently to summer temperatures when spring SWE is not considered. This could be the case if the energy limitations manifest as summer temperature for yellow cedar and growing-season length for the other two species, with mountain hemlock and Pacific silver fir experiencing a greater degree of summer water stress. There is a limited amount of experimental data to back up this claim as most physiological studies on yellow

cedar have been conducted on seedlings and clones with a focus on dehardening and frost hardiness. However, Puttonen and Arnott (1994) included temperature as a control on yellow cedar stecklings and found an independent effect of temperature on shoot growth. They also found that growth resumed quickly in warmer temperatures following a short cold spell given a long photoperiod, suggesting that temperatures can be a strong environmental control of yellow cedar growth.

Both mountain hemlock and Pacific silver fir show a climate response reminiscent of the high-elevation sites described by Peterson and Peterson (2001), with both growing-season temperature and spring SWE moderating growth, and both species show the negative relationship with maximum temperature from the prior year (Figure 5). This suggests that the sites are at an elevation where temperatures are one of the primary environmental factors that can limit tree growth (Körner, 2012). But regionally, the lack of summer precipitation can induce a water deficit that more strongly impacts annual growth (Stephenson, 1990). The VIC model has been successfully used in the arid Eastern Washington to identify biologically meaningful water stress parameters that impact growth more than precipitation, which generally falls during the dormant season (e.g., Restaino et al., 2016; Littell et al., 2008). But there is no consistent relationship between the three yellow cedar chronologies and either DEF or precipitation, and the relationships that do exist (i.e. positive relationship with growth and winter DEF) appear to be more a product of covariance between variables than a direct environmental control (Figure 5). This is not consistent with the majority of dendroecoogical studies in the region, which tend to show that summer water stress often moderates summer growth (e.g., Peterson and Peterson, 1994; Peterson et al., 2002; Case and Peterson, 2007). This could be a product of a failure in the VIC model to adequately capture evapotranspiration at these sites, and a lack of correlations with DEF does not imply that water stress is not important or not present for yellow cedar. One plausible explanation for a lesser impact of water streass at these sites relates to their topographic location. Each site has a northerly aspect, on a generally steep slope (Robertson, 2011). This would have a tendency to shield the trees from an excessive evaporative demand in the summer, as well as maintaining a higher soil moisture content throughout the summer. Although this inference suggests that tree growth at these sites may not be representative of yellow cedar throughout the region, it does show that yellow cedar at these sites are well suited for use as a regional temperature proxy.

At each site, PRISM temperatures can be successfully used to model tree growth, and the model

can be reversed to predict summer temperatures through time with a single predictor variable. The model has skill at predicting temperatures, performing better than random over the reconstruction period. The bootstrapped model statistics are encouraging as a validation of the temperature-growth relationship, more so because autocorrelation in the temperature and tree-ring series was not removed (Table 2). Retaining the autocorrelation in the time series might violate the assumption of independent residuals in a linear regression. Using bootstrapped model statistics avoids this issue by resampling the data. A positive CE and moderate R^2 of the reconstruction at each site are consistent with other tree-ring based temperature reconstructions at mid-latitude sites (e.g., Trouet et al., 2013; Wilson et al., 2016). The poorest performing model, Grouse Butte, included the one chronology that lacked the mid-20^{th} century decrease in growth (Figure 3), which appears to have been a real feature in the temperature data and globally (Anchukaitis et al., 2017). Temperature reconstructions modeled from the first PC of the three yellow cedar chronologies also perform well at these sites, showing that most of the shared variance in growth between the sites is related to regional climate variations, specifically temperature. Otherwise the temperature response seen at each site could have been attributed to local microclimate conditions rather than regional trends.

Reconstruction skill of the temperature model as applied throughout the region gives further credence to yellow cedar as a proxy for temperatures (Figure 7). The model has the most skill on the western slopes of the Cascades, as expected. A surprising result is the higher skill in the Puget Sound lowlands. Additional skill here cannot be attributed strictly to the proximity to meteorological station locations, as many long-term stations are located in the Cascade passes and elsewhere where the model is less skillful. Rather, the spatial pattern of model skill appears to coincide with regional climate zones (Mass, 2008). The poor-skill zone to the extreme western side of Washington is an area frequently inundated with marine air, low clouds, and an abundance of precipitation. Summer temperatures here would not be expected to track the variations on the leeward side of that mountain range (The Olympic Mountains), as cloud cover has a stronger effect on summer temperatures. Poor model skill to the east of the Cascade Mountains corresponds to a region of greater diurnal and seasonal temperature variability and a moderate influence from the continental climate regime, and confirms both the relationship between my sites and temperatures on the west slopes, and that temperature variations east of the Cascades do differ. As most existing temperature proxies represent the continental climate, which Eastern Washington more

closely resembles than do the western slopes, this reconstruction introduces a new look at regional temperature variability. However, the wide spread of model skill in a region represented by a single grid cell in most low-resolution climate models highlights the importance of high-resolution modeling in capturing the true range of variability in a region. Indeed, even within the spatial coverage of these high-resolution models small topographic differences can greatly influence climate and subsequent tree growth (Bunn et al., 2018).

This reconstruction shows a number of decadal to centennial-scale features that are consistent with other temperature reconstructions in North America. The yellow cedar reconstruction shows a number of brief periods where temperatures were above the 1951-1980 mean, but that these lasted for at most a decade with the exception of an extended warm period c1600 (Figure 8). The two warmest spikes in temperature occurred just prior to 1700 and c1800, and the late 17^{th} century spike was also captured by Graumlich and Brubaker (1986). The high temperature anomaly seen c1800 can be seen in two interior North America reconstructions by Luckman et al. (1997) and Wilson and Luckman (2003) but delayed by about a decade. A cool 19^{th} century is consistent with both Graumlich and Brubaker (1986) and Luckman et al. (1997), and with large-scale reconstructions such as the reconstruction ensemble published by the PAGES2K consortium (Pages 2K consortium, 2013) and the NTREND reconstruction (Anchukaitis et al., 2017). Volcanism in the early 1800s was evident in the chronologies, with the 1809-1810 boundry, corresponding to the "unknown" eruption of 1809, serving as a marker year for low growth at each of the sites and species Dai et al. (1991); Mosley-Thompson et al. (2003); Guevara-Murua et al. (2014). Where this reconstruction differs is primarily in the decadal-scale variability. A closer look at the NTREND reconstruction for the Pacific Northwest shows that the two agree throughout most of the record on a multi-decadal to centennial scale with the exception of the 16^{th} century (Figure 9), but higher frequency variability is simply not well represented. This is to be expected, as the proxy data used for the NTREND reconstruction are from the continental chronologies and are not directly subjected to the Pacific climate patterns. This is a valuable new look at more than 600 years of temperature variability west of the Cascades, and can add new information to these hemispheric reconstructions.

Conclusion

This work has shown that yellow cedar can be a useful proxy for temperature west of the Cascade mountains, potentially adding new and valuable information to both regional and hemispheric temperature reconstructions. Reconstructed temperatures from 1300-1900 do not reach the levels seen in the twentieth century, nor is there a period of sustained increase in temperatures seen at any other point in this record. Though the low-frequency trends in this reconstruction align well with other temperature reconstruction in the northern hemisphere, valuable new information that can be attributed to marine influences on climate can be gleamed from this reconstruction. But more work is needed to determine if the temperature-growth relationship exhibited among these sites is a feature seen in the species throughout the region, or if the local topography makes these chronologies unique in their usefulness as a temperature proxy. We also need to do more to determine if the climate signal is stable throughout the reconstruction. The later part of the twentieth century has seen an unprecedented increase in global temperatures, most notably in minimum temperature (IPCC, 2018). This is reflected in the real increase in yellow cedar growth over the same time period, but other climate-growth relationships in the region have been shown to diverge over the instrumental period (Marcinkowski et al., 2015, for example). Expanding the co-dominant chronologies to each of the three sites, and identifying suitable yellow cedar stands throughout the region for further sampling, should be undertaken to verify these results and potentially expand the network of yellow cedar throughout the region.

Literature Cited

Agee, J. K. and M. Vaughn. 1993. The Headwaters Old Growth of Canyon Lake Creek. Technical report, Trillium Corporation and Whatcom Community Land Trust, Bellingham, WA.

Anchukaitis, K. J. 2017. Tree Rings Reveal Climate Change Past , Present , and Future. *Proceeding of the American Philosophical Society* 161(3):244–263.

Anchukaitis, K. J., R. J. S. Wilson, K. R. Briffa, U. Büntgen, E. R. Cook, R. D. D'Arrigo, N. Davi, J. Esper, D. C. Frank, B. E. Gunnarson, G. C. Hegerl, S. Helama, S. Klesse, P. J. Krusic, H. W. Linderholm, V. Myglan, T. J. Osborn, P. Zhang, M. Rydval, L. Schneider, A. Schurer, G. C. Wiles, and E. Zorita. 2017. Last millennium Northern Hemisphere summer temperatures from tree rings: Part II, spatially resolved reconstructions. *Quaternary Science Reviews* 163:1–22.

Barrett, T. M. and R. R. Pattison. 2017. No evidence of recent (19952013) decrease of yellow-cedar in Alaska. *Canadian Journal of Forest Research* 47(1):97–105.

Beier, C. M., S. E. Sink, P. E. Hennon, D. V. D'Amore, and G. P. Juday. 2008. Twentieth-century warming and the dendroclimatology of declining yellow-cedar forests in southeastern Alaska. *Canadian Journal of Forest Research* 38(6):1319–1334.

Bidlack, A., S. Bisbing, B. Buma, D. V. D'Amore, P. E. Hennon, T. Heutte, J. Krapek, R. Mulvey, and L. Oakes. 2017. Alternative interpretation and scale-based context for "No evidence of recent (19952013) decrease of yellow-cedar in Alaska" (Barrett and Pattison 2017). *Canadian Journal of Forest Research* 47(1):1145–1151.

Biondi, F. and K. Waikul. 2004. DENDROCLIM2002: A C++ program for statistical calibration of climate signals in tree-ring chronologies. *Computers and Geosciences* 30(3):303–311.

Biondi, F., M. Hay, and S. Strachan. 2014. The tree-ring interpolation model (TRIM) and its application to Pinus monophylla chronologies in the Great Basin of North America. *Forestry* 87(4):582–597.

Bivand, R., T. Keitt, and B. Rowlingson. 2019. rgdal: Bindings for the 'Geospatial' Data Abstraction Library. R package version 1.4-3.

Bunn, A. G. 2008. A dendrochronology program library in R (dplR). *Dendrochronologia* 26(2):115–124.

Bunn, A. G. 2010. Statistical and visual crossdating in R using the dplR library. *Dendrochronologia* 28(4):251–258.

Bunn, A. G., M. W. Salzer, K. J. Anchukaitis, J. M. Bruening, and M. K. Hughes. 2018. Spatiotemporal variability in the climate growth response of high elevation bristlecone pine in the White Mountains of California. *Geophysical Research Letters* .

Buras, A. 2017. A comment on the expressed population signal. *Dendrochronologia* 44:130–132.

Case, M. J. and D. L. Peterson. 2007. Growth-climate relations of lodgepole pine in the North Cascades National Park, Washington. *Northwest Science* 81(1):62–75.

Coats, S., J. E. Smerdon, B. I. Cook, R. Seager, E. R. Cook, and K. J. Anchukaitis. 2016. Internal ocean-atmosphere variability drives megadroughts in Western North America. *Geophysical Research Letters* 43(18):9886–9894.

Cook, E. R. and L. A. Kairiukstis (editors) . 1990. Methods of Dendrochronology: applications in the environmental science. Kluwer Academic Publishers.

Cook, E. R., D. M. Meko, D. W. Stahle, and M. K. Cleaveland. 1999. Drought reconstructions for the continental United States. *Journal of Climate* 12(4):1145–1162.

Crown, D. J. and M. L. Parker. 1979. Densitometric analysis of wood from five Douglas-fir provenances. *Silvae Genetica* 28(2-3):48–53.

Dai, J., E. Mosley-Thompson, and L. G. Thompson. 1991. Ice Core Evidence for an Explosive Tropical Volcanic Eruption 6 Years Preceding Tambora. *Journal of Geophysical Research* 96(D9):17,361–17,366.

Daly, C., R. P. Neilson, and D. L. Phillips. 1994. A statistical-topographic model for mapping climatological precipitation over mountainous terrain. *Journal of Applied Meteorology* 33:140–158.

Daly, C., W. P. Gibson, G. H. Taylor, G. L. Johnson, and P. P. Pasteris. 2002. A knowledge-based approach to the statistical mapping of climate. *Climate Research* 22(2):99–113.

D'Arrigo, R. D., G. C. Jacoby, and R. M. Free. 1992. Tree-ring width and maximum latewood density at the North American tree line: parameters of climatic change. *Canadian Journal of Forest Research* 22(9):1290–1296.

Evans, M. E. K., D. A. Falk, A. Arizpe, T. L. Swetnam, F. Babst, and K. E. Holsinger. 2017. Fusing tree-ring and forest inventory data to infer influences on tree growth. *Ecosphere* 8(7).

Franklin, J. F. and C. T. Dyrness. 1973. Natural Vegetation of Oregon and Washington. Technical report, Pacific Northwest Forest and Range Experiment Station.

Franklin, J. F. and M. A. Hemstrom. 1981. Aspects of Succession in the Coniferous Forests of the Pacific Northwest. *In* Forest Sucession, H. H. Shugart and D. B. Botkin, editors, chapter 14, 212–229. Springer Advanced Textx in Life Sciences, Springer, New York, NY.

Fritts, H. C., J. E. Mosimann, and C. P. Bottorff. 1969. A revised computer program for standardizing tree-ring series. University of Arizona, Laboratory of Tree-Ring Research. *Tree-Ring Bulletin* 29(1-2):15–20.

Graumlich, L. J. and L. B. Brubaker. 1986. Reconstruction of annual temperature (1590-1979) for Longmire, Washington, derived from tree rings. *Quaternary Research* 25(2):223–234.

Guevara-Murua, A., C. A. Williams, E. J. Hendy, A. C. Rust, and K. V. Cashman. 2014. Observations of a stratospheric aerosol veil from a tropical volcanic eruption in December 1808: Is this the Unknown 1809 eruption? *Climate of the Past* 10(5):1707–1722.

Hamlet, A. F., P. Carrasco, J. Deems, M. M. Elsner, T. Kamstra, C. Lee, S.-Y. Lee, G. S. Mauger, E. P. Salathé, I. M. Tohver, and L. W. Binder. 2012. Final Report for the Columbia Basin Climate Change Scenarios Project. Technical report, Climate Impacts Group, Unversity of Washington, Seattle, WA.

Heeter, K. J., G. L. Harley, S. L. Van De Gevel, and P. B. White. 2019. Blue intensity as a temperature proxy in the eastern United States: A pilot study from a southern disjunct population of Picea rubens (Sarg.). *Dendrochronologia* 55:105–109.

Hegerl, G. C., T. J. Crowley, W. T. Hyde, and D. J. Frame. 2006. Climate sensitivity constrained by temperature reconstructions over the past seven centuries. *Nature* 440(7087):1029–1032.

Hennon, P. E., D. V. D'Amore, D. T. Wittwer, A. Johnson, P. G. Schaberg, G. J. Hawley, C. M. Beier, S. E. Sink, and G. P. Juday. 2006. Climate warming, reduced snow, and freezing injury could explain the demise of yellow-cedar in southeast Alaska, USA. *World Resource Review* 18(2):427–450.

Hennon, P. E., C. M. McKenzie, D. V. D'Amore, D. T. Wittwer, R. Mulvey, M. S. Lamb, F. E. Biles, and R. C. Cronn. 2016. A climate adaptation strategy for conservation and management of yellow-cedar in Alaska. Technical Report GTR-917, Pacific Northwest Research station, US Forest Service, Portland, OR.

Hijmans, R. J. 2019. raster: Geographic Data Analysis and Modeling. R package version 2.8-19.

IPCC. 2018. Global warming of 1.5C. An IPCC Special Report on the impacts of global warming of 1.5C above pre-industrial levels and related global greenhouse gas emission pathways, in the context of strengthening the global response to the threat of climate change,, volume In Press. Intergovernmental Panel on Climate Change.

Körner, C. 2012. Alpine Treelines. Springer Basel, Basel.

Kuhn, M., J. Wing, S. Weston, A. Williams, C. Keefer, A. Engelhardt, T. Cooper, Z. Mayer, B. Kenkel, R Core Team, M. Benesty, R. Lescarbeau, A. Ziem, L. Scrucca, Y. Tang, C. Candan, and T. Hunt. 2019. caret: Classification and Regression Training. R package version 6.0-84.

Kusnierczyk, E. R. and G. J. Ettl. 2002. Growth response of ponderosa pine (Pinus ponderosa) to climate in the eastern Cascade Mountains, Washington, U.S.A.: Implications for climatic change. *Ecoscience* 9(4):544–551.

LANDFIRE. 2014. Mean Fire Return Interval Layer.

Laroque, C. P. and D. J. Smith. 1999. Tree-ring analysis of yellow-cedar (Chamaecyparis nootkatensis) on Vancouver Island, British Columbia. *Canadian Journal of Forest Research* 29(1):115–123.

Liang, X., D. P. Lettenmaier, E. F. Wood, and S. J. Burges. 1994. A simple hydrologically based model of land surface water and energy fluxes for general circulation models. *Journal of Geophysical Research* 99(D7):14,415–14,428.

Littell, J. S., D. L. Peterson, and M. Tjoelker. 2008. Douglas-fir growth in mountain ecosystems: Water limits tree growth from stand to region. *Ecological Monographs* 78(3):349–368.

Luckman, B. H., K. R. Briffa, P. D. Jones, and F. H. Schweingruber. 1997. Tree-ring based reconstruction of summer temperatures at the Columbia Icefield, Alberta, Canada, AD 1073-1983. *Holocene* 7(4):375–389.

Marcinkowski, K., D. L. Peterson, and G. J. Ettl. 2015. Nonstationary temporal response of mountain hemlock growth to climatic variability in the North Cascade Range, Washington, USA. *Canadian Journal of Forest Research* 45(6):676–688.

Mass, C. 2008. The Weather of the Pacific Northwest. University of Washington Press, Seattle, WA.

Mosley-Thompson, E., T. A. Mashiotta, and L. G. Thompson. 2003. High resolution ice core records of late holocene volcanism: Current and future contributions from the Greenland PARCA cores. *Geophysical Monograph Series* 139:153–164.

Pages 2K consortium. 2013. Continental-scale temperature variability during the past two millennia. *Nature Geoscience* 6(5):339–346.

Pebesma, E. J. and R. S. Bivand. 2005. Classes and methods for spatial data in R. *R News* 5(2):9–13.

Peterson, D. W. and D. L. Peterson. 2001. Mountain hemlock growth responds to climatic variability at annual and decadal time scales. *Ecology* 82(12):3330–3345.

Peterson, D. W., D. L. Peterson, and G. J. Ettl. 2002. Growth responses of subalpine fir to climatic variability in the Pacific Northwest. *Canadian Journal of Forest Research* 32(9):1503–1517.

Peterson, D. W. L. and D. W. L. Peterson. 1994. Effects of climate on radial growth of subalpine conifers in the North Cascade Mountains. *Canadian Journal of Forest Research* 24(9):1921–1932.

Pierce, D. 2019. ncdf4: Interface to Unidata netCDF (Version 4 or Earlier) Format Data Files. R package version 1.16.1.

PRISM Climate Group. 2019. Oregon State University, http://prism.oregonstate.edu. Created October 13, 2017.

Puttonen, P. and J. T. Arnott. 1994. Influence of photoperiod and temperature on growth, gas exchange, and cold hardiness of yellow cypress stecklings. *Canadian Journal of Forest Research* 24(8):1608–1616.

QGIS Development Team. 2018. QGIS Geographic Information System.

R Core Team. 2019. R: A Language and Environment for Statistical Computing. R Foundation for Statistical Computing, Vienna, Austria.

Razavi, S. and R. Vogel. 2018. Prewhitening of hydroclimatic time series? Implications for inferred change and variability across time scales. *Journal of Hydrology* 557:109–115.

Restaino, C. M., D. L. Peterson, J. S. Littell, and M. G. Turner. 2016. Increased water deficit decreases Douglas fir growth throughout western US forests. *Proceedings of the National Academy of Sciences* 113(34):9557–9562.

Robertson, C. S. 2011. Dendroclimatology of yellow cedar (Callitropsis nootkatensis) in the Pacific Northwest of North America. Masters thesis, Western Washington University.

RStudio Team. 2015. RStudio: Integrated Development Environment for R. RStudio, Inc., Boston, MA.

Salzer, M. W., M. K. Hughes, A. G. Bunn, and K. F. Kipfmueller. 2009. Recent unprecedented tree-ring growth in bristlecone pine at the highest elevations and possible causes. *Proceedings of the National Academy of Sciences* 106(48):20,348–53.

Schurer, A. P., S. F. B. Tett, and G. C. Hegerl. 2014. Small influence of solar variability on climate over the past millennium. *Nature Geoscience* 7(2):104–108.

St. George, S. 2014. An overview of tree-ring width records across the Northern Hemisphere. *Quaternary Science Reviews* 95:132–150.

Stephenson, N. L. 1990. Climatic Control of Vegetation Distribution: The Role of the Water Balance. *The American Naturalist* 135(5):649–670.

Stephenson, N. L. 1998. Actual evapotranspiration and deficit: Biologically meaningful correlates of vegetation distribution across spatial scales. *Journal of Biogeography* 25(5):855–870.

Stokes, M. A. and T. L. Smiley. 1968. An Introduction to Tree-Ring Dating. The University of Arizona Press, Tuscon, AZ.

Trouet, V., H. F. Diaz, E. R. Wahl, A. E. Viau, R. Graham, N. E. Graham, and E. R. Cook. 2013. A 1500-year reconstruction of annual mean temperature for temperate North America on decadal-to-multidecadal time scales. *Environmental Research Letters* 8(2).

Warren, W. G. 1980. On Removing the Growth Trend From Dendrochronological Data. *Tree-Ring Bulletin* 40:35–44.

Wickham, H. 2016. ggplot2: Elegant Graphics for Data Analysis. Springer-Verlag New York.

Wickham, H., R. Franois, L. Henry, and K. Mller. 2019. dplyr: A Grammar of Data Manipulation. R package version 0.8.0.1.

Williams, A. P., J. Michaelsen, S. W. Leavitt, and C. J. Still. 2010. Using tree rings to predict the response of tree growth to climate change in the continental United States during the twenty-first century. *Earth Interactions* 14(19):1–20.

Wilson, R. J. S. and B. H. Luckman. 2002. Tree-ring reconstruction of maximum and minimum temperatures and the diurnal temperature range in British Columbia, Canada. *Dendrochronologia* 20(3):257–268.

Wilson, R. J. S. and B. H. Luckman. 2003. Dendroclimatic reconstruction of maximum summer temperatures from upper treeline sites in Interior British Columbia, Canada. *The Holocene* 13(6):851–861.

Wilson, R. J. S., K. J. Anchukaitis, K. R. Briffa, U. Büntgen, E. R. Cook, R. D. D'Arrigo, N. Davi, J. Esper, D. C. Frank, B. E. Gunnarson, G. C. Hegerl, S. Helama, S. Klesse, P. J. Krusic, H. W. Linderholm, V. Myglan, T. J. Osborn, M. Rydval, L. Schneider, A. Schurer, G. C. Wiles, P. Zhang, and E. Zorita. 2016. Last millennium northern hemisphere summer temperatures from tree rings: Part I: The long term context. *Quaternary Science Reviews* 134:1–18.

Zang, C. and F. Biondi. 2015. Treeclim: An R package for the numerical calibration of proxy-climate relationships. *Ecography* 38(4):431–436.

Appendix I: Programs and Packages

The following is a list of the programs and packages used in this analysis. This list is comprehensive with respect to the published analysis, though other programs may have been used during the investigative stage. Following the program list are the associated references.

QGIS version 3.6.2 (QGIS Development Team, 2018)

R program for statistical analysis, version 3.6.0 (R Core Team, 2019)

R Studio, version 1.2.1335 (RStudio Team, 2015)

R packages:

- dplR version 1.6.9 (Bunn, 2008)
- sp version 1.3.1 (Pebesma and Bivand, 2005)
- raster version 2.8-19 (Hijmans, 2019)
- ggplot2 version 3.3.1 (Wickham, 2016)
- rgdal version 1.4-3 (Bivand et al., 2019)
- caret version 6.0-84 (Kuhn et al., 2019)
- ncdf4 version 1.16.1 (Pierce, 2019)
- dplyr version 0.8.0.1 (Wickham et al., 2019)
- treeclim version 2.0.3 (Zang and Biondi, 2015)